

Baryon asymmetry at the weak phase transition in presence of arbitrary CP violation.

E. Torrente Lujan.

Inst. fur Theoretische Physik, Universitat Bern
Sidlerstrasse 5, 3012 Bern, Switzerland.
e-mail: e.torrente@cern.ch

Abstract

We consider interactions of fermions with the domain wall bubbles produced during a first order phase transition. A new exact solution of the Dirac equations is obtained for a wall profile incorporating a position dependent CP violating phase. The reflection coefficients are computed, a resonance effect is uncovered for rapidly varying phases. This resonance effect happens when the energy and mass of the incident particles are $E/m = \Delta\theta/2$. Where $\Delta\theta$ is the phase variation across the wall width. We calculate the chiral charge flux through the wall surface and the corresponding baryon asymmetry of the Universe. It agrees in sign and magnitude with the observed baryonic excess $\rho_B/s \approx 10^{-10}$ for a large range of parameters and CP violation. As a function of $\Delta\theta$, the ratio ρ_b/s reach a maximum for $\Delta\theta \approx 2 - 4\pi$ and $m \approx m_{top}$.

PACS: 11.27.+d, 03.65.-w, 02.30.Hq, 02.30.Gp, 11.30.Fs, 98.80.Cq

1 Introduction

During the last few years, a considerable amount of work has been dedicated to the possibility of generating a sizeable baryon asymmetry on the electro-weak phase transition (see for example [1, 2, 3, 4]). For an excess of baryons to develop in an Universe which initially has zero baryon number, the already well known following conditions, first enunciated by Sakharov, must be met: 1) Some interaction of elementary particles must violate baryon number. 2) C and CP must be violated in order that there is not a perfect equality between rates of $\Delta B \neq 0$ processes, since otherwise no asymmetry could evolve from an initially symmetric state. 3) A departure from thermal equilibrium must play an essential role, since otherwise CPT would assure compensation between processes increasing and decreasing the baryon number. Remarkably, the standard model of weak interactions may provide all these conditions. In particular the third one can be met if the weak phase transition is at least weakly first order.

In a first order phase transition, the conversion from one phase to the other occurs through nucleation. This happens when the system is either supercooled or superheated. Bubbles of the "true" phase (with an expectation value of some Higgs field $v \neq 0$) expand rapidly absorbing the region of the "false" phase ($v = 0$). At the bubble surface there is a region or "wall", in principle of microscopic dimensions, which separates the phases.

The speed regime of the expanding bubble walls is poorly understood in the theory. After an acceleration period, the final stationary speed of the expanding bubble walls could be anywhere in the range $0.1 - 0.9 c$ [5]. Lattice and numerical simulations indicate that $v_{wall} \approx 0.5$ can be reached in circumstances of high latent heat and high surface tension which could be achieved in the minimal supersymmetric standard model (MSSM) for realistic Higgs masses $M_H < \approx M_W$. For having even higher wall speed $v_{wall} \approx 0.9$, it is necessary some fine tuning (a extremely low value for the friction parameter, see [6]). At later stages of the bubble evolution an oscillatory regime with successive periods of expansion and contraction is naturally expected [6].

Particles in the "false" (higher temperature) phase are reflected off the advancing bubble walls, while most particles in the low temperature phase are unable to catch up with the receding walls, and cannot equilibrate across the phase boundary. Thus one has a departure from equilibrium and a baryon asymmetry can be generated.

In the physical conditions of the early Universe the fermions moving through the bubble wall will interact also with the particles in the surrounding plasma, a full transport problem must be considered. A useful simplifying assumption is to decompose the process into two steps, one describing the production of the CP asymmetry on the transmission/reflection coefficients when the quarks/antiquarks are scattered on the wall, the second describing the transport and the eventual transformation of the CP asymmetry into a baryon asymmetry via the baryon number anomaly.

Assuming that the scattering from the wall is little affected by diffusion corrections, the effects of the surrounding plasma can be partially incorporated by introducing a Higgs field effective potential which takes into account finite temperature corrections to the tree-level potential. The structure and profile of the wall depends on this effective potential

on a complicated way. Fermions passing through the domain wall acquire a mass which is proportional to the vacuum expectation value (VEV) of the Higgs field, which is determined from the equations of motion of the finite temperature effective action of the bubble. The problem of computation of transmission coefficients reduces to the solution of a Dirac equation with a space dependent mass term. Exact solutions has been obtained only for two simple cases: for a wall profile approximated by a step function [4, 7] and for an average Higgs field profile of the "kink ansatz" type [3](with z , a coordinate perpendicular to the wall):

$$\phi(z) \propto \left(1 + \tanh\left(\frac{z}{\delta}\right)\right) \quad (1)$$

where the width of the wall is given essentially by the inverse of the Higgs mass:

$$\delta = \frac{\sqrt{2}}{M_H} \quad (2)$$

In this ansatz there is not variation of the complex phase of the Higgs field through the wall. It has been examined in [8] the effect of introducing a small CP-violating imaginary part in Eq.(1) as a perturbative effect. Numerical solutions have been obtained for some more complicated profiles which incorporate locally dependent complex phases and which are considered to be "reasonable" enough although not necessarily solution of any equation of motion (for example in [9]).

The object of this work is the computation of transmission coefficients of a fermion in a certain fixed Higgs field background with an arbitrary, possibly high, complex phase. With them we will be able to estimate the baryon asymmetry of the universe.

Consider a langrangian for the fermion Ψ in the background of a complex scalar with a Yukawa coupling. For the scalar to have a nonzero complex vacuum expectation value, we can assume it is a part of an extended Higgs sector such as MSSM or a more general two Higgs-doublets model. The fermionic part of the lagrangian important to us is

$$L_\Psi = \bar{\Psi}_L i \not{\partial} \Psi_L + \bar{\Psi}_R i \not{\partial} \Psi_R - h \bar{\Psi}_L \Psi_R \phi - h^* \bar{\Psi}_R \Psi_L \phi^* \quad (3)$$

with Yukawa coupling constant h . Ψ acquires a position dependent mass, which, in a appropriate reference frame is a function only of one coordinate , $m(z) = h \langle \phi(z) \rangle$. From L_Ψ the equations of motion are obtained

$$\begin{aligned} i \not{\partial} \Psi_L - m^* \Psi_R &= 0 \\ i \not{\partial} \Psi_R - m \Psi_L &= 0 \end{aligned} \quad (4)$$

It is possible to absorb a constant phase in $m(z)$ with a redefinition of one of the chiral fields.

One needs only the plane wave solution of the Dirac equation for particles moving along the normal to the wall profile (considered microscopically flat). For any other incoming direction, the problem can be reduced to the latter performing a Lorentz boost. Reordering

the spinorial components, the Dirac operator given by Eqs.(4) can be factorized into 2×2 blocks. For solutions with positive energy E , we can make the ansatz:

$$\Psi = e^{-iEt+ip_t \cdot x_t} \begin{pmatrix} \psi_I(z) \\ \psi_{II}(z) \end{pmatrix} \equiv e^{-iEt+ip_t \cdot x_t} \begin{pmatrix} \psi_1 \\ \psi_3 \\ \psi_4 \\ \psi_2 \end{pmatrix} \quad (5)$$

Where x_t , is the projection onto the x-y plane. ψ_1 and ψ_2 are eigenspinors of the chirality operator, γ_5 , for the eigenvalue $+1$ and ψ_3, ψ_4 for -1 . Going through an intermediate Lorentz transformation we obtain finally the two equations

$$(i\partial_z + Q(z))\psi_I = 0 \quad (6)$$

$$(i\partial_z + Q^*(z))\psi_{II} = 0 \quad (7)$$

With

$$Q(z) = \begin{pmatrix} E_l & -m(z) \\ m(z)^* & -E_l \end{pmatrix}; \quad E_l = +\sqrt{E^2 - p_t^2} \quad (8)$$

We will deal in this work with the particular case given by the function

$$m(z) = \begin{cases} m_0 \exp i(-\Delta\theta\lambda z) \exp -\lambda z & \text{if } z > 0 \\ m_0 & \text{if } z \leq 0 \end{cases} \quad (9)$$

The constants $\Delta\theta, \lambda$ are real; $\lambda > 0$; m_0 can be also set to real without loss of generality. This function represents a linear phase variation with a global difference of $\Delta\theta$ over a distance of the order of the wall thickness defined by $\delta \equiv 1/\lambda$. In specific models $\Delta\theta$ can be related to the quantity of CP violation in the Higgs sector. The position dependent complex phase can be considered as an additional source of effective CP-violating phenomena.

The profile of the wall given by $m(z)$ cannot be derived from any classical field equations in presence of an effective Higgs potential with up to quartic terms as it is usually considered. It can be trivially seen however that such a wall profile corresponds to an energy density of the wall per unit area of the form

$$\mathcal{E}(\Delta\theta) - \mathcal{E}(0) = \lambda m_0^2 \Delta\theta^2 \quad (10)$$

with $\mathcal{E}(0)$ of the same order of magnitude as the energy density of the "kink" ansatz (1). Some indication can be obtained from the previous formula. As the nucleation temperature $T_n \propto \mathcal{E}$ (see Eq.(13) in [10]) and according to Table (1) in [6] which relates nucleation rates and wall speed, a high value for $\Delta\theta$ would favor generically a lower value for the wall speed. In this work we will see (Fig.(6)(C-D)) that, for small wall speed, a high value for $\Delta\theta$ is equally acceptable as a lower one in order to obtain a reasonable ρ_B/s ratio.

2 Solving the Dirac equation.

It would be possible to solve Eqs.(6-7) with the function given by Eq.(9), reducing them to a Bessel-like differential equation. It is possible and advantageous however to use perturbation theory to compute the evolution operator of the system. The summation to all orders of the perturbation expansion is possible thanks to the special form of $Q(z)$. There are two main advantages in doing so: the first one is that the procedure is easily generalizable to any number of dimensions (for example to incorporate mixing between generations), the second one is that the evolution operator is computed directly and the reflection coefficients are easily given in terms of its components. A similar technique has been used already in [11, 12] to compute the neutrino oscillation probabilities in solar matter.

The evolution operator of the differential system (6) is given by the path-ordered integral

$$U(z, z_0) = P \exp i \int_{z_0}^z dz Q(z) \quad (11)$$

In this work we are concerned with an operator Q of the form

$$Q = Q^0 + V(z) \quad (12)$$

With

$$Q^0 = \begin{pmatrix} E & 0 \\ 0 & -E \end{pmatrix}; \quad V = \begin{pmatrix} 0 & -k \exp -\sigma z \\ k \exp -\sigma^* z & 0 \end{pmatrix} \quad (13)$$

k real, σ complex in general. The real part of σ is greater than zero. It will be set $\Re\sigma = 1$ without loss of generality.

Formally, it is possible to solve Eq.(11) by successive iterations:

$$U(z, z_0) = U^{(0)}(z, z_0) + \sum_{n=1}^{\infty} U^{(n)}(z, z_0); \quad U^{(0)}(z, z_0) = \exp \left(i Q^0 (z - z_0) \right) \quad (14)$$

$U^{(n)}$ is the well-known integral

$$U^{(n)} = i^n \int_{\Gamma} dz_n \dots dz_1 U^0(z, z_n) V(z_n) \dots U^0(z_2, z_1) V(z_1) U^0(z_1, z_0) \quad (15)$$

The domain of integration is defined by

$$\Gamma \equiv z > z_n > \dots > z_1 > z_0.$$

Following the same arguments as in [11] one can show that it is enough to compute U in the $z \rightarrow \infty$ limit. The evolution for finite z can be deduced from the expression for this limit. Through elementary manipulations of Eq.(15), we get the elements of $U^{(n)}$ in a basis of eigenvectors of Q^0 :

$$\begin{aligned} \langle b | U^{(n)} | a \rangle &= i^n \exp(i(Q_b^0 z - Q_a^0 z_0)) \times \\ &\times \sum_{k_1, \dots, k_{(n-1)}} \int_{\Gamma} d^n \tau \exp(i z_n w_{bk_1} + \dots + i z_1 w_{k_{(n-1)}a}) V_{bk_1}(z_n) \dots V_{k_{(n-1)}a}(z_1) \end{aligned} \quad (16)$$

With $w_{k_1 k_2} = Q_{k_1}^0 - Q_{k_2}^0$. Q_k^0 one of the two eigenvalues of Q^0 .

Due to the dimensionality of the problem and the special form for V , the summatory in Eq.(16) either is zero or reduces to only one term depending on whether n is odd or even and on the states a, b . For diagonal terms ($a = b$) the product of $V \dots V$ is always zero when n is odd. When n is even there is a single surviving term. For non-diagonal terms, the situation is reversed: the only one surviving term appears for n odd. This single remaining term is always of the alternating form $\dots V_{12} V_{21} V_{12} \dots$. So,

$$\langle b | U^{(n)} | a \rangle = i^n \exp(i(Q_b^0 z - Q_a^0 z_0)) I_{ab}^{(n)} \times \begin{cases} (-|k|)^{n/2} & a = b \\ V_{ba} (-|k|)^{(n-1)/2} & a \neq b \end{cases} \quad (17)$$

All the functions appearing in the integral $I_{ab}^{(n)}$ are of exponential type, the following equality [11] can be applied:

$$\begin{aligned} I_n(w_1, \dots, w_n) &\equiv \int_{z_0}^{\infty} \dots \int_{z_0}^{x_2} dx_n \dots dx_1 \exp \sum_n w_n x_n \\ &= \frac{(-1)^n \exp(z_0 \sum_n w_n)}{w_1(w_1 + w_2) \dots (w_1 + w_2 \dots + w_n)} \\ &\quad (\text{valid if } \Re w_n < 0, \forall n) \end{aligned} \quad (18)$$

In our case the sums in the denominator of Eq.(18) are of the form

$$\begin{aligned} w_1 + w_2 + \dots + w_j &= iw_{bk_1} - L + iw_{k_1 k_2} - L^* + \dots + iw_{k(j-1)k_j} - L \\ &= iw_{bk_j} + n_1 L + n_2 L^* \end{aligned} \quad (19)$$

$w_{bk(j)}$ can take only the values $\{0, \pm 2E\}$. L is σ or σ^* . One have for the integers n_1, n_2 : $n_1 + n_2 = j$ $n_1 = n_2$ or $n_1 = n_2 \pm 1$; they are equal or differ in one unit.

For the diagonal terms, $a = b$, n even (writing $s = 2Ei - \sigma$):

$$\begin{aligned} I_{aa}^{(n), \text{even}} &= \frac{\exp z_0(n/2)(s + s^*)}{s^*(s^* + s)(s^* + s + s^*) \dots ((n/2)(s + s^*))} \\ &= \frac{\exp z_0(n/2)(s + s^*)}{\prod_{j=2, \text{even}}^n (j/2)(s + s^*) \prod_{j=1, \text{odd}}^{n-1} [s^* + (j-1)(s + s^*)/2]} \\ &= \frac{\exp z_0(n/2)(s + s^*)}{(s + s^*)^{n/2} (\frac{n}{2})! (s + s^*)^{n/2} \prod_{l=1}^{n/2} [s^*/(s + s^*) + (l-1)]} \\ &= \frac{\exp z_0(n/2)(s + s^*)}{(s + s^*)^n (\frac{n}{2})! [s^*/(s + s^*)]_{(n/2)}} \end{aligned} \quad (20)$$

For non-diagonal terms, taking $a = 1, b = 2$ to simplify the notation:

$$I_{ab}^{(n), \text{odd}} = \frac{(-1) \exp z_0((n/2)(s + s^*) + s^*)}{s^*(s^* + s)(s^* + s + s^*) \dots ((n/2)(s + s^*) + s^*)}$$

$$\begin{aligned}
&= \frac{(-1) \exp z_0(n/2)(s + s^*)}{\prod_{j=2, \text{even}}^{n-1} (j/2)(s + s^*) \prod_{j=1, \text{odd}}^n (s^* + (j-1)(s + s^*)/2)} \\
&= \frac{(-1) \exp z_0(n/2)(s + s^*)}{(s + s^*)^{(n-1)/2} \left(\frac{n-1}{2}\right)! (s + s^*)^{(n+1)/2} \prod_{l=1}^{(n+1)/2} [s^*/(s + s^*) + (l-1)]} \\
&= \frac{(-1) \exp z_0(n/2)(s + s^*)}{(s + s^*)^n \left(\frac{n-1}{2}\right)! [s^*/(s + s^*)]_{(n+1)/2}} \tag{21}
\end{aligned}$$

We have used the Pochhammer symbol defined by Eq. (49).

So, inserting Eqs.(20,21) in Eq.(17) and taking $s + s^* = -2$, $z_0 = 0$:

$$\begin{aligned}
\langle 1 | U | 1 \rangle &= \\
&= e^{iEz} \left(1 + \sum_{n=2, \text{even}}^{\infty} i^n (-k^2)^{n/2} \frac{1}{(-2)^n \left(\frac{n}{2}\right)! [-s^*/2]_{(n/2)}} \right) \\
&= e^{iEz} \left(1 + \sum_{m=1}^{\infty} \left(\frac{k^2}{4}\right)^m \frac{1}{m! [-s^*/2]_{(m)}} \right) \\
&= e^{iEz} {}_0F_1 \left(-\frac{s^*}{2}; \frac{k^2}{4} \right) \tag{22}
\end{aligned}$$

$$\begin{aligned}
\langle 1 | U | 2 \rangle &= \\
&= e^{iEz} k \sum_{n=1, \text{odd}}^{\infty} i^n (-k^2)^{(n-1)/2} \frac{(-1)}{(-2)^n \left(\frac{n-1}{2}\right)! [-s^*/2]_{((n+1)/2)}} \\
&= e^{iEz} \frac{-2ik}{k^2} \sum_{m=1}^{\infty} \left(\frac{k^2}{4}\right)^m \frac{1}{(m-1)! [-s^*/2]_{(m)}} \\
&= e^{iEz} \frac{-ik}{s^*} {}_0F_1 \left(1 - \frac{s^*}{2}; \frac{k^2}{4} \right) \tag{23}
\end{aligned}$$

and similarly for the other two matrix elements.

$$\langle 2 | U | 2 \rangle = e^{-iEz} {}_0F_1 \left(-\frac{s}{2}; \frac{k^2}{4} \right) \tag{24}$$

$$\langle 2 | U | 1 \rangle = e^{-iEz} \frac{ik}{s} {}_0F_1 \left(1 - \frac{s}{2}; \frac{k^2}{4} \right) \tag{25}$$

The matrix U can be written as

$$U(z \rightarrow \infty, z_0) = \exp iQ_0(z - z_0) U_{red}(z_0)$$

$$U_{red}(z_0) = \begin{pmatrix} F & G \\ G^* & F^* \end{pmatrix} \tag{26}$$

writing $\sigma = \lambda(1 + i\Delta\theta)$, $k = m_0/\lambda$, $E = E_l/\lambda$

$$\begin{aligned} G &= \frac{-im_0/\lambda}{1 + (2E_l/\lambda - \Delta\theta)i} {}_0F_1 \left(\frac{3}{2} + \left(\frac{E_l}{\lambda} - \frac{\Delta\theta}{2} \right) i; \frac{m_0^2}{4\lambda^2} \right) \\ F &= {}_0F_1 \left(\frac{1}{2} + \left(\frac{E_l}{\lambda} - \frac{\Delta\theta}{2} \right) i; \frac{m_0^2}{4\lambda^2} \right) \end{aligned} \quad (27)$$

In the case $z_0 \neq 0$, F, G would include a factor $\exp -2z_0$ in its argument. The special case $E_l/\lambda = \Delta\theta/2$ will be important later. In this case F, G become dependent only on m_0 and have the explicit simple form:

$$\begin{aligned} G &= -i \frac{m_0}{\lambda} {}_0F_1 \left(\frac{3}{2}; \frac{m_0^2}{4\lambda^2} \right) = -i \sinh \left(\frac{m_0}{\lambda} \right) \\ F &= {}_0F_1 \left(\frac{1}{2}; \frac{m_0^2}{4\lambda^2} \right) = \cosh \left(\frac{m_0}{\lambda} \right) \end{aligned} \quad (28)$$

To obtain \bar{U} , evolution operator for the Eq.(7), one must make the change $\Delta\theta \rightarrow -\Delta\theta$. The matrix become

$$\begin{aligned} \bar{U}(z \rightarrow \infty, z_0) &= \exp iQ_0(z - z_0) \bar{U}_{red}(z_0) \\ \bar{U}_{red}(z_0) &= \begin{pmatrix} \bar{F} & \bar{G} \\ \bar{G}^* & \bar{F}^* \end{pmatrix} \end{aligned} \quad (29)$$

with

$$\begin{aligned} \bar{G} &= \frac{-im_0/\lambda}{1 + (2E_l/\lambda + \Delta\theta)i} {}_0F_1 \left(\frac{3}{2} + \left(\frac{E_l}{\lambda} + \frac{\Delta\theta}{2} \right) i; \frac{m_0^2}{4\lambda^2} \right) \\ \bar{F} &= {}_0F_1 \left(\frac{1}{2} + \left(\frac{E_l}{\lambda} + \frac{\Delta\theta}{2} \right) i; \frac{m_0^2}{4\lambda^2} \right) \end{aligned} \quad (30)$$

See Appendix A for some new formulas for the absolute values of generalized hypergeometric functions which can be obtained from the general properties of U, \bar{U} .

Following the same reasoning used in [11], using the general properties of the evolution operator, the evolution for any finite z is given by the matrix

$$U(z, z_0) \equiv U_s(z)^{-1} U_s(z_0) = U_{red}^{-1}(z) e^{iQ_0(z-z_0)} U_{red}(z_0) \quad (31)$$

In this work, we will make use only of the infinite z limit.

3 The reflection Coefficients.

We will follow the same procedure as in [1] for defining the reflection coefficient. As it can be seen directly from Eqs.(26,29), in the region $z \rightarrow \infty$ we have the following asymptotic behavior

$$\begin{aligned}\psi_2(\infty), \psi_3(\infty) &\simeq e^{-iE_l z} \\ \psi_1(\infty), \psi_4(\infty) &\simeq e^{iE_l z}\end{aligned}\quad (32)$$

In this region, the eigenspinors ψ_2, ψ_3 correspond to, vanishing mass, left-moving particles of opposite chirality and similarly ψ_1, ψ_4 to right moving particles.

For left-moving particles incident from the symmetric phase two components coexist at $z \rightarrow \infty$, the incident particle itself and the reflected one by the domain wall. We define asymptotic reflection coefficients R, \bar{R} as

$$\psi_1(\infty) = R\psi_3(\infty); \quad \psi_4(\infty) = \bar{R}\psi_2(\infty) \quad (33)$$

The momentum eigenstates for $z < 0$ are obtained diagonalizing the constant matrix $Q(0)$. The eigenvectors

$$\psi_{\pm} = \frac{1}{\lambda} \begin{pmatrix} m_0 \\ E_l - p_{\pm} \end{pmatrix} \quad (34)$$

correspond to right moving (+) and left moving particles (-) with respective eigenvalues $p_{\pm} = \pm p_l = \pm \sqrt{E_l^2 - m_0^2}$.

Imposing the boundary condition that at $z < 0$ only a left-moving particle with momentum p_- propagates, the wave function at infinite is:

$$\psi(\infty) = U(z \rightarrow \infty, 0)\psi_- \quad (35)$$

The reflection coefficient R is given explicitly by the expression

$$R = \frac{U_{11} + tU_{12}}{U_{21} + tU_{22}} = e^{2E_l z_i} \frac{F + tG}{G^* + tF^*}; \quad t = (E_l + p_l)/m_0 \quad (36)$$

and similarly for \bar{R} .

We are interested in the asymmetry between the reflection probabilities: $A = |R|^2 - |\bar{R}|^2$. In the ultrarelativistic limit ($E_l/m_0 \gg 1$), $R \rightarrow F^*/G$. In the limit $E/m_0 \rightarrow 1$ ($t \rightarrow 1$), both reflection coefficients $|R|, |\bar{R}| \rightarrow 1$ and the asymmetry $A \rightarrow 0$. It is straightforward to check that in the case we had supposed from the beginning a complex constant mass m_0 , the quantities R, \bar{R} would remain independent of the phase of m_0 taking into account the formula (36).

In Fig.(1) the asymmetry A is plotted as a function of the dimensionless quantity E_l/m_0 and some fixed values of $\Delta\theta$. For $\Delta\theta = \pi$ (plot B) the results obtained here coincide with the numerical result obtained in [1] (Fig. 2). For a realistic case where $\lambda \sim M_H \sim M_W$ and $m_0 \sim m_{top}$, the value of $\mu \equiv m_0\delta \equiv m_0/\lambda \approx 2 - 2.5$. For this range of μ (continuous curves in Fig.(1)) the asymmetry A is non-negligible for a large E/m_0 range. In general A is negligible for fermion masses corresponding to $\mu < \approx 10^{-1}$ which can be translated to the condition $m_0 < \approx 2m_{bottom}$ for not so heavy Higgs masses.

As the phase difference $\Delta\theta$ increases, the height of the peaks keeps roughly unaltered but their position moves:

$$(E_l/m_0)_{peak} = |\Delta\theta|/2\mu.$$

For large differences $E_l/m_0 - \Delta\theta/2\mu$, \bar{R} becomes negligible and the asymmetry $A \sim |R|^2$. \bar{R} is non-negligible only for E/m_0 and $\Delta\theta$ small enough, such that the imaginary part of the first parameter of the Hypergeometric function in Eqs.(27) approaches zero.

For higher values of $\Delta\theta$ some resonant effect becomes apparent, the peaks get sharper and the asymmetry is only non-negligible around them. This is particularly evident in the last plot (D). This effect could lead to an essentially monochromatic asymmetry in scenarios with highly oscillatory or random phase differences. For high $\Delta\theta$, the asymmetry quantity can be approximated by the expression

$$A \approx \delta(E_l/m_0 - \Delta\theta/2\mu) f(\mu, \Delta\theta) \quad (37)$$

where $\delta(x)$ is a delta-like peaked function and $f(\mu, \Delta\mu)$, the value of A at peak, is easily computable from Eqs.(28), it is of interest only its general behavior:

$$f(\mu, \Delta\theta) \rightarrow \begin{cases} \mu^2/2\Delta\theta & \text{for } \mu \rightarrow 0 \\ 1 & \text{for } \mu \rightarrow \infty \end{cases} \quad (38)$$

The resonant behavior is again evident in Fig.(2) where we plot A as a function of the parameter $\Delta\theta$ for various μ as before. The peaks in the asymmetry function appear for values such that $\Delta\theta_{peak} = 2E_l\delta$.

4 Chiral charge flux through the bubble wall and the Baryon asymmetry.

The chiral charge flux in front of the wall in the symmetric phase and in the wall frame is given by [1]:

$$F = \frac{1}{2\pi^2\gamma} \int_0^\infty dp_l \int_0^\infty p_t dp_t (f^s(-p_l, p_t) - f^b(p_l, p_t)) A(m_0, \lambda, p_l) \quad (39)$$

A is the asymptotic asymmetry defined in the previous section and the thermal equilibrium fermion flux densities f^s, f^b in the symmetric and broken phases respectively (neglecting Fermi blocking factors) are:

$$f^s = \frac{(p_l/E^s)}{\exp(\gamma(E^s - up_l)/T) + 1}, \quad E^s = \sqrt{p_l^2 + p_t^2}$$

$$f^b = \frac{(p_l/E^b)}{\exp(\gamma(E^b + up_l)/T) + 1}, \quad E^b = \sqrt{p_l^2 + p_t^2 + m_0^2}$$

The wall velocity in the fluid frame is given by u ; $\gamma = 1/\sqrt{1-u^2}$; p_l, p_t are the longitudinal and transverse momentum of the fermion with respect to the wall. T is the equilibrium temperature. The use of asymptotic expressions for f^s and A is questionable, the position dependent mass implies the existence of a density gradient even at thermal equilibrium. The Formula (39) would be valid at far distances from the wall and in absence of inter-particle collisions. We can expect that the formula is reasonable valid as long as the wall width is small compared to the mean free path in the plasma, so effects inside the wall do not play an important role.

Defining dimensionless momentum and wall width $p_l/m_0 = x; p_t/m_0 = y, \epsilon = T/\lambda$, defining also $\kappa = \mu\gamma/\epsilon$ and integrating with respect p_t , we arrive to the expression:

$$F = T^3 \frac{\mu^2}{2\pi^2 \gamma^2 \epsilon^2} F^*(\mu, \kappa, u) \quad (40)$$

Where F^* is the function defined by the integral:

$$F^*(\mu, \kappa, u) = \int_0^\infty dx x A(\mu, x) \left(\log \frac{1 + \exp(-\kappa(1-u)x)}{1 + \exp(-\kappa\sqrt{1+x^2} - \kappa ux)} \right) \quad (41)$$

The dependence with the CP violating phase $\Delta\theta$ is fully contained in the asymmetry $A(\mu, x)$. The integrand in Eq.(41) is defined positive if $u > 0$. For negative u (as it could happen in late wall contraction phases) its sign changes at a certain $x_0 = 1/(2\sqrt{u^2 + |u|})$. For large x the integrand multiplying A in Eq.(41) approaches zero exponentially for any value of the parameters, the most important contribution to the integral comes from the values of $A(x)$ with x relatively small. This implies that in the case F^* might become negative, its absolute value would be relatively small. It is expected that the resonance observed in the previous section tends to be washed out due to this behavior: the resonance in A appears at large x , just when the rest of the integrand is exponentially smaller. The resonance in A could have a more significant effect in non-equilibrium cases: for flux densities f^s, f^b with large tails at large momentum.

We plot in Fig.(3) the chiral flux divided by the cubic temperature given by the Eqs.(40-41) as a function of u . F/T^3 is rather independent of u and $\Delta\theta$ in the logarithmic scale of the figure, except for $u \rightarrow 1$. It is however strongly dependent in μ , it changes a few orders of magnitude for μ varying changing in the range $1 - 10^{-1}$.

For large $\Delta\theta$, using the formula (37), one obtains the approximate expression for the integral F^* :

$$F^* \approx f(\mu, \Delta\theta) \log \frac{1 + \exp(-\kappa(1-u)\sqrt{(\Delta\theta/2\mu)^2 - 1})}{1 + \exp(-\kappa(\Delta\theta/2\mu + u\sqrt{(\Delta\theta/2\mu)^2 - 1}))} \quad (42)$$

For a large value of $\Delta\theta$ but keeping the quantity $\kappa\Delta\theta/2\mu \equiv \gamma\Delta\theta/2\epsilon$ relatively small, F^* , and so F , are proportional to $\Delta\theta$

$$F^* = \frac{\kappa(1+u)}{2} f(\mu, \Delta\theta) \frac{\Delta\theta}{2\mu} \quad (43)$$

This behavior coincides essentially with the proportionality in $\Delta\theta$ obtained in [13].

In the opposite regime, for a large quantity $\kappa\Delta\theta/2\mu$, F^* approaches zero exponentially:

$$F^* \approx 2f(\mu, \Delta\theta)e^{-\kappa\Delta\theta/2\mu} \sinh(\kappa u\Delta\theta/2\mu) \quad (44)$$

We plot F^* as a function of $\Delta\theta$ in Figs.(4) (given by the the exact Formula (41)). The small and large $\Delta\theta$ behavior observed in the figure are clearly given by the Eqs.(45-43) respectively. It is interesting to compare Fig.(4) with Fig.(2). In agreement with what was expected from the form of the integral (41), the resonances are lost here. However, It remains still a non obvious remarkable behavior. F^* (and then ρ_b/s to be defined later) is $\propto \Delta\theta$ in a surprisingly sizeable range. after reaching a maximum for $\Delta\theta$ around $2 - 4\pi$ for practically any value of the rest of the parameters, F^* goes quickly to zero for higher values.

4.0.1 The baryon asymmetry

The baryon asymmetry/entropy ratio of the Universe through the sphaleron process is given in the charge transport scenario with two Higgs doublets by [1]:

$$\frac{\rho_B}{s} = \frac{4}{5} \frac{\Gamma_B}{T} \frac{\tau}{u} \frac{F}{s} \quad (45)$$

Where

- Γ_B is the sphaleron transition rate per unit of volume in the symmetric phase [14]:

$$\Gamma_B \simeq 3\eta\alpha_w^4 T^4 \quad (46)$$

with an unknown numerical factor $\eta \approx 0.1 - 1$ [15]. Note however that a violation rate $\sim O(\alpha_w^5 T^4)$ has been proposed recently [16]. The introduction of an additional factor α_w would not change greatly the final results, or at least its order of magnitude, but it is an indication of the global incertitude still existing on Γ_B .

- τ is a typical transport time within which the scattered fermions are captured by the wall and in which they can be converted into baryon number [1] $\tau \simeq l/u$ with l the mean free path of the corresponding particle. In some works τ is computed numerically [1]. We will parametrize it in the form

$$l = \frac{D}{T}$$

D can be interpreted as a diffusion-like constant with a magnitude in the order $D \approx 1 - 20$ (for example $D \approx 4 - 6$ in [17, 14]).

- The entropy density is given by $s = 2\pi^2 g_* T^3/45$ with $g_* \approx 100$, the effective degrees of freedom of the relativistic particles at the electroweak phase transition.

- F is the charge flux given by Eq.(40) which contains all the dependence on $\Delta\theta$ through the integral F^* .

Inserting all the factors the baryon/entropy ratio is given explicitly by:

$$\frac{\rho_B}{s} \approx 5 \cdot 10^{-9} \times (\eta D) \times \frac{\mu^2 F^*}{u^2 \epsilon^2 \gamma^2} \quad (47)$$

F^* is a function only of the adimensional parameters ϵ, μ, u and $\Delta\theta$. The explicit dependence with the temperature T has vanished in this formulation. The range of validity of Eq.(45) is limited by the simplicity of charge transport model. It should be valid for $\Gamma_B \tau / T^3 \ll u$ ([1]) or $\eta D \ll 10^6 u^2$. With $\eta \approx 1, D \approx 10$, we would have then the condition $u \gg 10^{-2}$. In the other extreme the formula lack a priori validity for $u \rightarrow 1$. In this case there is not time for the fermion in front of the wall to thermalize and the flux densities defined in the previously can not be used. For those cases a detailed Boltzman transport treatment should be performed instead. Note however that, according to previous arguments taking into account the dependence of A at large momentum, the thermal case would act as a lower limit. Another constraint comes from the condition for the validity of formula (39): the wall width should be smaller that the mean free path of the fermion or $\epsilon = T/\lambda \lesssim D$.

The matter content of the observed universe is given by $\rho_B/s \simeq 10^{-10}$ (from nucleosynthesis calculations, see [1] and references therein). Figure (5) shows the ratio ρ_B/s . For large u , ρ_B/s follows the behavior of F: decreases and approaches zero for $u \rightarrow 1$. For small u , as long as the equation is still valid, the divergent behavior $\sim 1/u^2$ is apparent. According to Fig.(5) a value $\rho_b/s \approx 10^{-10}$ may be explained by this mechanism for weak scale baryogenesis for a wide range of parameters, including a large variation in the rather unknown product ηD , as long as $\mu \sim 0.5 - 2$. μ is the main parameter needed to be tuned.

In Figure (6) the same ρ_b/s is plotted as a function of negative wall speed (contracting wall case). In agreement with previous considerations ρ_B/s is of opposite sign in this case and relatively smaller in absolute value. The effect is more important for $\mu \approx 1 - 2$, $\Delta\theta$ large and medium speeds. Note that the pattern of the μ dependence is different here than that one appearing in Fig.(5). For a detailed knowledge of the final ρ_B/s an integration over the full history of the bubble may be necessary.

The dependence with the adimensional thickness of the wall ($\epsilon = T/\lambda$) is shown in Fig.(7) (cf. with Fig.(4) in [1]). ϵ corresponds approximately to the inverse Higgs mass scale and should be independent of T ($\lambda \sim T$) in most models. The dependence is rather modest for thin walls ($\epsilon < 1$). For relatively thicker walls $\epsilon > 5 - 10$ the suppression is very important: values as $\rho_B/s \ll 10^{-11}$ are reached in this region.

The dependence with the CP violating phase $\Delta\theta$ of ρ_b/s is contained totally in F^* and appears in Fig.(4). Although interesting qualitatively, it is clear from a numerical point of view that the maximum variation, a factor 4 from $\Delta\theta \approx \pi/2$ to $\Delta\theta \approx 2\pi$, is still small in comparison with all the other incertitudes appearing in the present knowledge, observational and theoretical, of ρ_b/s . An important conclusion from Fig.(4) is that, although decreasing, ρ_b/s still keeps the right order of magnitude even for very large $\Delta\theta$.

5 Summary and conclusions

As conclusion, we were able to solve the Dirac equation with a space dependent complex mass term which, although not a solution of the equations of motion, reproduces the expected variation in module and in complex phase of the average Higgs field across the wall. From the solution of the Dirac equation the particle-antiparticle transmission asymmetry is computed. The analytical results presented here confirm previous numerical computations for small $\Delta\theta$ and predict an unexpected behavior for highly oscillatory phase fields.

We have computed the chiral flux and the baryon asymmetry. For a large set of parameters this is compatible with the "experimental" value $\rho_B/s \sim 10^{-10}$. This is true even for extremely large values of CP violation $\Delta\theta$. The resulting baryon asymmetry for contracting walls has been estimated for the first time to our knowledge.

The main uncertainties come from the rate of anomalous baryon number violation at high temperature and from the method itself. In view of the dependence on ϵ and $\Delta\theta$, It is clear that the plausibility of this model depends only on the existence of a massive fermion (as the Top quark) and is rather independent of the values of the Higgs mass and the critical temperature of the weak transition as long as they keep in a reasonable range.

A more detailed microscopic treatment based in the Boltzman equation is clearly advisable. The solution of the Dirac equation obtained here is particularly suitable for this purpose. Although the mass term which has been used is somehow artificial, is a suitable toy model to study large CP violation environments. This solution can be used as a starting point to obtain numerical correction for more realistic mass fluctuations.

The method used here can be used with little modifications to solve the Dirac equation for a purely local dependent phase mass term ($\lambda \rightarrow 0, \Delta\theta\lambda \neq 0$ in Eq.(9) or equivalently σ purely imaginary in Eq.(13)). In order to circumvent convergence problems this must be done taking the limit $\Re\lambda \rightarrow 0$ in the finite propagation time Eq.(31).

A Appendix: some old and new formulas about Hypergeometric Functions

The generalized Hypergeometric function [18] is defined by

$${}_pF_q(a_1, \dots, a_p, b_1, \dots, b_q; z) = \sum_{n=0}^{\infty} \frac{(a_1)_{(n)} \dots (a_p)_{(n)} z^n}{(b_1)_{(n)} \dots (b_q)_{(n)} n!} \quad (48)$$

where the Pochhammer symbol is

$$(z)_{(n)} = \Gamma(n+z)/\Gamma(z) \quad (49)$$

in particular

$${}_0F_1(b; z) = \sum_{n=0}^{\infty} \frac{1}{(b)_{(n)}} \frac{z^n}{n!} \quad (50)$$

The derivative of ${}_0F_1$ is again a ${}_0F_1$ function:

$$\frac{d {}_0F_1(\gamma; z)}{dz} = \frac{1}{\gamma} {}_0F_1(1 + \gamma; z) \quad (51)$$

The function ${}_0F_1$ is related to the Bessel Functions by the formula

$$J_n(z) = \frac{(z/2)^n}{\Gamma(1+n)} {}_0F_1\left(1+n; -\frac{z^2}{4}\right) \quad (52)$$

For a Q as given by Eq.(12) is traceless, $\det Q(z, z_0) = \det Q(0, 0) = 1$, or $|F|^2 - |G|^2 = 1$. The formulas (27) are valid for any $E, \Delta\theta$ real, k complex, we obtain:

$$\left| {}_0F_1\left(\frac{1}{2} + \epsilon i; x^2\right) \right|^2 - \frac{x^2}{|1/2 + \epsilon i|^2} \left| {}_0F_1\left(\frac{3}{2} + \epsilon i; x^2\right) \right|^2 = 1 \quad (53)$$

to be compared with the similar formulas obtained in [11] for the absolute values of the generalized hypergeometric functions ${}_nF_n$.

In fact, with little changes, one could compute U for any general matrix V with diagonal terms equal to zero and non-diagonal terms of general exponential type not necessarily equal. In the particular case of V hermitic: $V_{12} = V_{21}^* = k$, U_{red} is unitary and of the form

$$U_{red}(z_0) = \begin{pmatrix} \overline{F} & \overline{G} \\ -\overline{G}^* & \overline{F}^* \end{pmatrix} \quad (54)$$

with $\overline{F}, \overline{G}$ given by Eq.(29).

By the unitarity of the matrix (54), $|F|^2 + |G|^2 = 1$. And we get the formula:

$$\left| J_{-\frac{1}{2} + \epsilon i}(x) \right|^2 + \left| J_{\frac{1}{2} + \epsilon i}(x) \right|^2 = \frac{2 \cosh \pi \epsilon}{\pi x} \quad (55)$$

For $\epsilon = 0$ this formula reduces to the trigonometric case involving the well known Bessel functions of order $1/2$: $J_{-1/2}(x) = \sqrt{2/(\pi x)} \cos(x)$; $J_{1/2}(x) = \sqrt{2/(\pi x)} \sin(x)$.

Acknowledgments.

The author would like to thank to Peter Minkowski for many enlightening discussions. This work has been supported in part by the Wolffman-Nageli Foundation (Switzerland) and by the MEC-CYCIT (Spain).

References

- [1] A. Nelson, D. Kaplan, and A. Cohen, Nucl. Phys. B **373**, 453 (1992).
- [2] D. Toussaint, S. Treiman, F. Wilzek, and A. Zee, Phys. Rev. D. **19**, 1036 (1979).
- [3] A. Ayala, J. Jalilian-Marian, and L. McLerran, Phys. Rev. D. **49**, 5559 (1994).
- [4] G. Farrar and M. Shaposhnikov, Phys. Rev. Lett. **70**, 2833 (1993).
- [5] A. Dine, R. Leigh, P. Huet, A. Linde, and D. Linde, Phys. Lett. B. **283**, 219 (1992).
- [6] H. Kurki-Suonio and M. Laine, Phys. Rev. Lett. **77**, 3951 (1996).
- [7] M. Gavela, M. Lozano, J. Orloff, and O. Pene, Nucl. Phys. B **430**, 345 (1994).
- [8] K. Funakubo, A. Kakuto, S. Otsuki, S. Toyoda, and K. Takenaga, Prog. of Theo. Phys. **95**, 1067 (1995).
- [9] A. Cohen, D. Kaplan, and A. Nelson, Nucl. Phys. B **349**, 727 (1991).
- [10] M. Abney, hep-ph/9606476 .
- [11] E. Torrente-Lujan, Phys. Rev. D. **53**, 53 (1996).
- [12] E. Torrente-Lujan, hep-ph/9602398 .
- [13] K. Funakubo, A. Kakuto, S. Otsuki, and S. Toyoda, Prog. of Theo. Phys. **95**, 929 (1995).
- [14] A. Cohen, D. Kaplan, and A. Nelson, Ann.Rev.Nucl.Part.Sci **43**, 27 (1993).
- [15] J. Ambjorn and K. Farakos, Phys. Lett. B. **294**, 248 (1992).
- [16] P. Arnold, D. Son, and G. Yaffe, hep-ph/9609481 .
- [17] G. Bonini, hep-ph/9607406 .
- [18] I. Gradshteyn and I. Ryzhik, *Table of Integrals, series and products*, Academic Press, 1980.

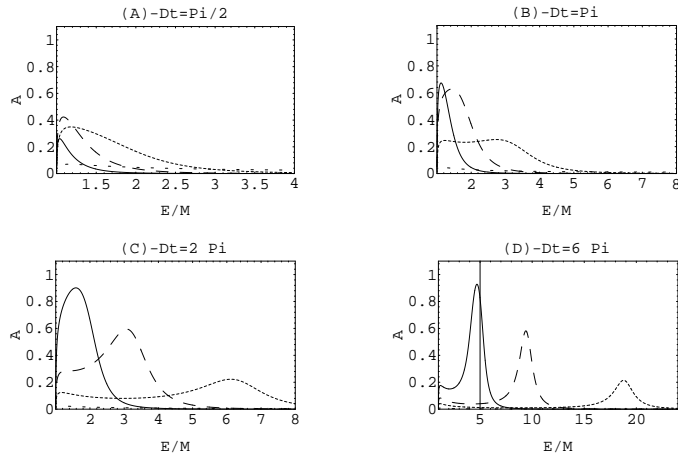


Figure 1: The asymmetry A as a function of E_l/m_0 . Continuous line: $\mu = 2$, dashed lines: respectively $\mu = 1, 1/2, 1/10$. From A to D: $\Delta\theta = \pi/2, \pi, 2\pi, 6\pi$.

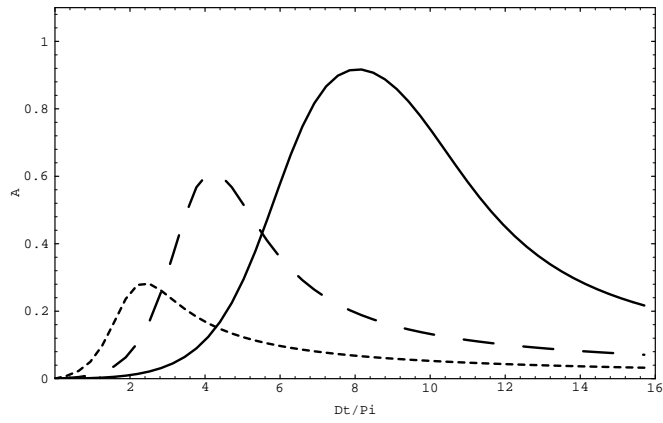


Figure 2: Asymmetry A as a function of $\Delta\theta$ and different μ as before. For each curve, the energy is chosen as $E_l/m_0 = 2$.

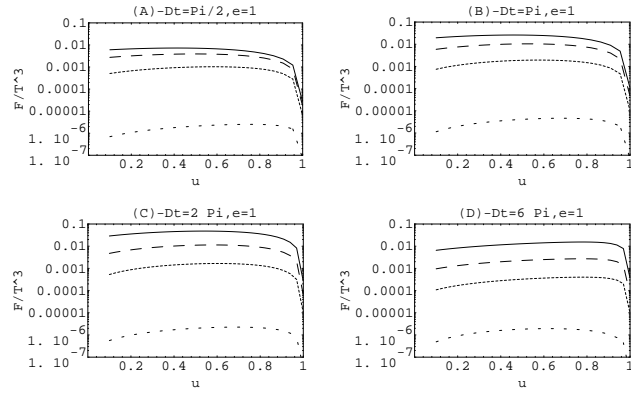


Figure 3: Chiral charge flux (Eq.(40)) as a function of the wall velocity u , for several $\Delta\theta$ and μ (continuous and dashed lines as in previous figures). In all the figures the adimensional wall width $\epsilon = 1$.

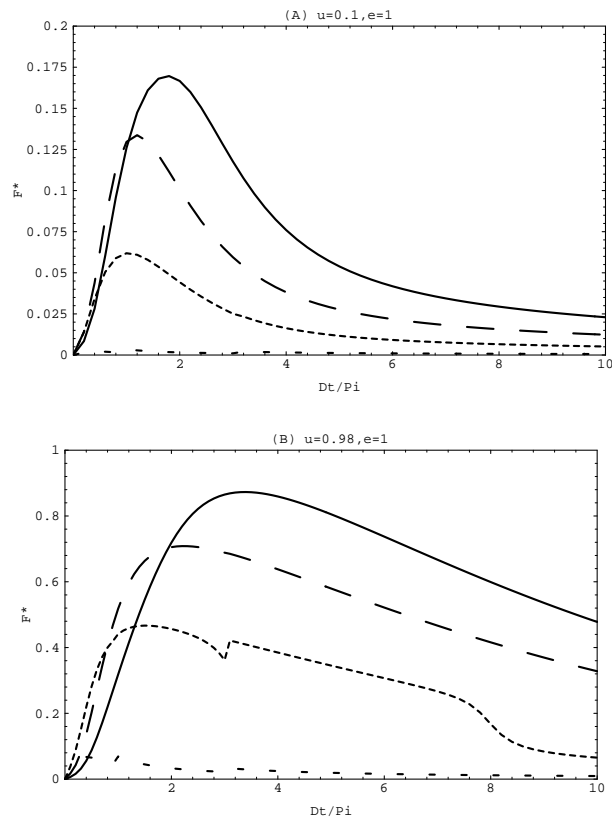


Figure 4: Dependence with $\Delta\theta$ for different μ ratios.

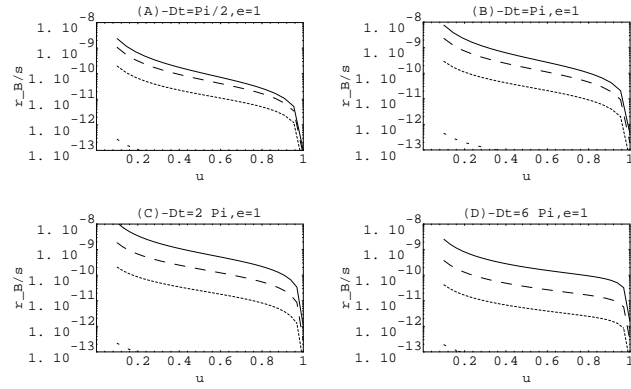


Figure 5: ρ_B/s ratio (Eq.(47), $\eta D = 1$) as a function of the wall velocity u (see explanation for the previous figure).

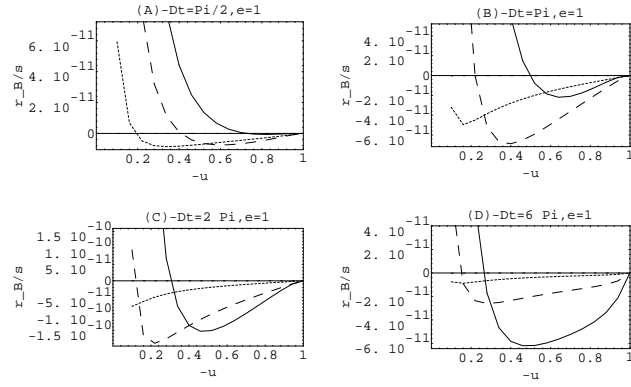


Figure 6: ρ_B/s ratio , (Eq.(47), $\eta D = 1$) for negative wall speeds (contracting walls).

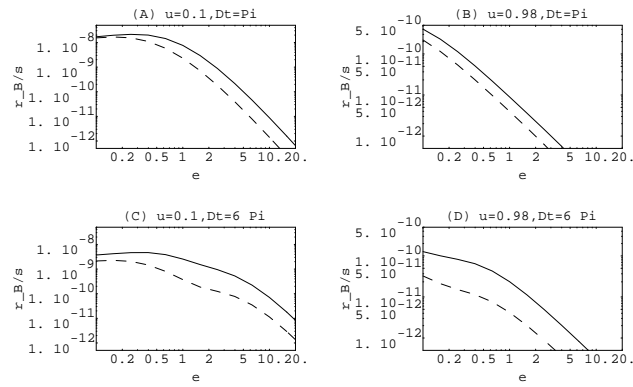


Figure 7: Dependence with the thickness of the wall $\epsilon = T/\lambda$. For high and low values of the wall velocity and $\Delta\theta$. Continuous line: $\mu = 2$, dashed line $\mu = 1$.